INTERNATIONAL JOURNAL OF CIRCUIT THEORY AND APPLICATIONS
Int. J. Circ. Theor. Appl. 2015; **43**:1209–1225
Published online 9 May 2014 in Wiley Online Library (wileyonlinelibrary.com). DOI: 10.1002/cta.1999

Distributed power flow loss minimization control for future grid

Kiyoshi Nakayama[1,*,†], Changhong Zhao[2], Lubomir F. Bic[1], Michael B. Dillencourt[1] and Jack Brouwer[3]

[1]*Department of Computer Science, University of California, Irvine, CA 92697-3435, USA*
[2]*Department of Electrical Engineering, California Institute of Technology, Pasadena, CA 91125-0001, USA*
[3]*Department of Mechanical and Aerospace Engineering, University of California, Irvine, CA 92697-3550, USA*

SUMMARY

In this paper, a novel decentralized algorithm is proposed to minimize power flow loss in a large-scale future grid connecting with many real-time-distributed generation systems by which power flows bi-directionally. The DC-power loss at each link is defined as the product of resistance and the square of current that can be considered as a quadratic flow cost. We employ the notion of tie-sets that reduces the complexity of the power flow loss problem by dividing a power network into a set of loops that forms a linear vector space on which the power loss problem can be formulated as a convex optimization problem. As finding a solution in each tie-set enables global optimization, we realize parallel computing within a system of independent tie-sets by integrating autonomous agents. Simulation results demonstrate the minimization of the power loss on every link by iteratively optimized power flows and show the superiority against the traditional centralized optimization scheme. Copyright © 2014 John Wiley & Sons, Ltd.

Received 24 December 2013; Revised 28 February 2014; Accepted 7 April 2014

KEY WORDS: power loss; DC-power flow; smart grid; distributed energy resource; distributed control; tie-set graph theory

1. INTRODUCTION

Future power networks will likely support bi-directional flow of electricity and include power production from multiple, disparate, and uncontrollable sources because of a high penetration of distributed renewable energy resources [1, 2]. Effective use of renewable resources can be realized by grid topology, controls, and optimization that can handle the dispersed and uncontrollable sources while minimizing the transmission and distribution losses, which offsets the dependence on fossil fuels. In addition, local autonomy is required because of communication times that are longer than those required to communicate grid perturbations and actuate hardware to prevent widespread outages. Local authority regimes also contain disparate policy and market frameworks in which the optimization and control infrastructure must operate. For these reasons, development of an autonomous distributed architecture that can minimize the power flow losses when distributing energy resources to consumers is required in a future large-scale power grid connecting with many real-time-distributed generation systems.

The topology of today's grids must be modified to integrate and manage distributed energy resources (DERs) on the grid. Current grid topology allows only one-way power flow, typically with a 'tree' structure in the distribution system. However, the tree topology will not hold anymore when DERs will be integrated into the grid because the topology is the worst not only in power loss but also in

*Correspondence to: Kiyoshi Nakayama, Department of Computer Science, University of California, Irvine, CA 92697-3435, USA.
†E-mail: kiyoshi.nakayama@ieee.org

communication delay as the number of hops between nodes grows in the order of the size of the network [3, 4]. While an interconnected or meshed network would provide higher reliability and flexibility, such meshed power networks are only found in a few urban areas. Nonetheless, attention has been focused on mesh topologies for development of new grid infrastructure because of the increased flexibility, efficiency, and resiliency they provide and the familiarity, good understanding, and technology associated with the analogous information and communications network of the Internet [5]. The benefit of using meshed networks also lies in preventing the grid from being isolated with each other in the event of a failure, natural disaster, or required maintenance. Besides those factors, it has also been studied how the minimum power loss in a power system is related to its network topology [6]. In the later part of simulation, we assessed how much power loss we can reduce by outputting random resistance and current value on each link and comparing the result using a mesh topology with the one using a tree topology to motivate the use and design of mesh topological grids.

As in Kirchhoff's laws, a set of loops called 'tie-sets' has been used in circuits and power systems demonstrating the effectiveness in controlling power flows and designing reliable systems even in a complicated non-planar graph [7, 8]. Although it is hard to give universal values for power flow loss (path loss) because many factors influence it (overhead or underground cables, type of cables, loading, weather, etc.), we focus on the nature of power loss that is proportionate to the product of the square of current and resistance on a link (the distance and thickness) [9–11]. As the power loss at a link has a quadratic flow cost, the problem can be formulated as a convex optimization problem. Our decentralized algorithm utilizes the notion of tie-sets that reduces the complexity of the power flow loss problem by dividing a power network into a set of loops that is considered a linear vector space where the power loss function can be simply formulated and solved. As finding a solution at each tie-set enables us to reach global optimization [12], we realize parallel computing based on tie-sets by integrating autonomous agents; the power loss on every link can be minimized with iterative optimization within a system of independent tie-sets. After minimizing the power loss by calculating optimal link currents within a tie-set, the minimized lost power is being injected at destination nodes. Hence, minimizing total power loss on lines also minimizes the additional power injection needed for the entire network. We show through simulation results that the proposed method realizes the minimization of the power flow loss on every link by optimized power flows and is superior to the traditional centralized optimization scheme.

2. RELATED WORK

Many efforts have been made in the domain of power loss minimization (PLM) as in [13] even before the development of communications systems that are being integrated into the power systems domain now. Power flow loss minimization for current power systems is discussed in [10, 11]. Stevenson [11] basically presents voltage control methods to improve the voltage level of a power system whilst minimizing losses. As in the work, the optimal power flow (OPF) problem classically is nonlinear and non-convex aiming to minimize the power generation costs and transmission loss in a power network. It has been subject to physical constraints based on Kirchhoff's and Ohm's law [13–15].

In the past decade, devising efficient algorithms with guaranteed performance has been much attention for the OPF problem. For example, nonlinear interior-point algorithms for an equivalent current injection model of the problem have recently proposed in [16] and [17].

A recent work of Jiang *et al*. [18] has improved implementation of the automatic differentiation technique for the OPF problem. To convexify the OPF problem, Jabr [19] justifies that the load flow problem of a radial distribution system can be modeled as a convex optimization problem in the form of a conic program. To overcome the nonlinearity, the majority of these works focus on linearization and approximation schemes to simplify the OPF. Christie *et al*. [20], for example, simplify the OPF problem by the small angle approximation. Some other relaxation methods can be found in [21, 22]. However, because of the presence of arctangent equality constraints, those results struggle to hold for a meshed network [23].

DOI: 10.1002/cta

A recent work by Lavaei *et al*. also proves that a closely related problem of finding an optimal operating point of a radiating antenna circuit is an nondeterministic polynomial time (NP)-complete problem, by reducing the number-partitioning problem to the antenna problem [24]. In [25], the DC OPF problem that minimizes the power loss in an electrical network is proposed by optimizing the voltage and power delivered at the network nodes. Tan *et al*. [25] study the direct current special case by leveraging recent developments on the zero duality gap of OPF [26] and presents a decentralized algorithm based on updating primal–dual variables. In [25, 26], the OPF problems are non-convex constrained quadratic programming problems. When zero duality gap holds between OPF and its dual, the original OPF can be achieved by solving the dual, which is convex.

Different from prior work on decentralized algorithms for OPF, for example, [25], which mainly focus on updating nodal variables like voltage and dual variables attached to nodes, in this paper, we design a decentralized algorithm based on updating the loop variables. The problem we are solving here, by making certain assumptions with our model, is a convex quadratic programming problem with linear constraints because M of (8) in Section 3.3 is a positive semi-definite matrix. Lavaei and Low [6] imply that a practical PLM problem is likely to be solvable using a convex algorithm. Generally, our method is efficient and costs less computational time given the sparse structure of power grids; that is, the number of fundamental tie-sets is in the same order as the number of nodes. By focusing on the notion of tie-sets, we can effectively divide the grid and form a μ-dimensional linear vector space.[‡] Our objective is to find an optimal flow that minimizes the power flow line losses in a meshed power network with distributed computations. We formulate the PLM problem on the basis of the currents, which has been a common formulation in circuits and systems and also is applicable to the future power systems. It is elegantly formulated with tie-set currents defined in Section 3.3, which have played significant role in circuits and systems [8].

3. PROBLEM FORMULATION

3.1. Power loss minimization problem

We consider a power network in which the line losses and loads are all resistive. Consequently, all voltages and currents are in phase and are represented by their root-mean-square values only. The network and its operating conditions are specified by a group $S=(V,E,I,C,R)$, where $V=(v_k, k=1,\ldots,n)$ is the set of vertices, $E=(e_k, k=1,\ldots,m)$ is the set of links (lines), $I=(i_k, k=1,\ldots,m)$ is the vector of link currents, $C=(c_k, k=1,\ldots,m)$ is the vector of link current capacities, and $R=(r_k, k=1,\ldots,m)$ is the vector of link resistances. Suppose the links are directed, with arbitrarily defined directions. When the current i_k flows along the direction of link e_k, then $i_k>0$; otherwise, $i_k<0$.

The power loss $p(i_k)$ on a link e_k is

$$p(i_k) = r_k {i_k}^2 \quad (-c_k \le i_k \le c_k), \tag{1}$$

and the power loss P_G of an entire graph is given by the sum of the power losses on all the links:

$$P_G = \sum_{e_k \in E} p(i_k) = I^T R^d I, \tag{2}$$

where $R^d = \mathrm{diag}(r_1, r_2, \ldots, r_m)$ is a diagonal matrix whose elements are resistances r_k. The PLM problem can be considered as an optimization problem over the current vector I. Note that power systems are usually controlled by changing the power injections at the vertices instead of directly controlling the currents. However, to convey the idea of PLM, we select the link currents as the variable. In implementation, currents can be controlled via, for example, controlling the voltages at the vertices.

[‡] μ is the nullity of a graph as defined in Section 3.2.1.

DOI: 10.1002/cta

We assume constant current injections $J \in \mathbb{R}^n$ at the vertices v_k, $k = 1, \ldots, n$. The link currents I should satisfy the current injection constraints imposed by J. Let A be the $n \times m$ incidence matrix, with $A_{kj} = 1$ if vertex v_k is the source of link e_j, -1 if vertex v_k is the sink of link e_j, and 0 otherwise. Then, we have

$$AI = J. \tag{3}$$

By [27], if the graph is a mesh (not a tree), given J, there is a subspace of solutions I to (3). Our objective is to find the solution I that minimizes the power loss P_G in (2) as follows.

Given C and R, the PLM problem is

$$\min_I P_{\mathrm{G}} = I^T R^d I \tag{4}$$

$$\text{s. t.} \quad -C \le I \le C. \tag{5}$$

To develop a decentralized algorithm to solve this problem using the tie-set theory, we convert P_G as a function of tie-set currents as shown in the following section.

3.2. Tie-set graph theory

Tie-set graph theory is proposed in [12,28] and used in many applications such as [29, 30]; we provide its brief review.

3.2.1. Fundamental system of tie-sets. For a given graph $G = (V, E)$ with a set of vertices $V = \{v_1, v_2, \ldots, v_n\}$ and a set of edges $E = \{e_1, e_2, \ldots, e_m\}$, let $L_i = \left\{e_1^i, e_2^i, \ldots\right\}$ be a set of all the edges that constitutes a loop in G. The set of edges L_i is called a tie-set [8]. Let T and $\overline{T}$ respectively be a spanning tree and a co-tree of G, where $\overline{T} = E - T$. $\mu = \mu(G) = \left|\overline{T}\right|$ is called the *nullity* of a graph. As T on a graph $G = (V, E)$ is a spanning tree, T does not include any tie-set. In other words, for $l \in \overline{T}$, $T \cup \{l\}$ includes one tie-set. Focusing on a subgraph $G_T = (V, T)$ of G and an edge $l = (a, b) \in \overline{T}$, there exists only one elementary path $P_T(b, a) \subseteq T$ whose origin is b and terminal is a in G_T. Then, a *fundamental tie-set* that consists of the path P_T and the edge $l = (a, b)$ is uniquely determined as

$$L(l) = \{l\} \cup P_T(b, a). \tag{6}$$

It is known that μ fundamental tie-sets exist in G, and they are called a *fundamental system of tie-sets*. If G is bi-connected, a fundamental system of tie-sets $\mathbb{L}_B = \left\{L_1, , L_2, \ldots, , L_\mu\right\}$ guarantees that it covers all the vertices and edges of G as shown in Figure 1. Even though a given graph is non-planar, a fundamental system of tie-sets creates a set of μ-independent loops as seen in Figure 6.

3.2.2. Independency of tie-sets. Any tie-set in a fundamental system of tie-sets is independent of each other. That is, any tie-set cannot be obtained by calculus $\oplus$[§] among other tie-sets. As $l \in \overline{T}$ is only included in a fundamental tie-set $L(l)$ of a fundamental system of tie-sets $\mathbb{L}_B$, a tie-set that includes l cannot be created even if the calculus $\oplus$ is applied to other fundamental tie-sets than $L(l)$. For any $\left\{L(l_i), L\left(l_j\right)\right\} \subseteq \mathbb{L}_B$, $\left(l_i \neq l_j\right)$, if $L(l_i) \cap L(l_j) \neq \varnothing$, a tie-set $L'(l_i)$ replaced by $L'(l_i) \leftarrow L(l_i) \oplus L(l_j)$ is also independent of other fundamental tie-sets. This transformation of a tie-set is carried out by the calculus $\oplus$ and called *L-transformation*.

There are systems of independent tie-sets that do not correspond to any fundamental systems of tie-sets constructed by spanning trees of a graph. In Figure 2, the tie-sets $\{L_1, L_2, L_3, L_4, L_5, L_6\}$ of the network on the left side forms a fundamental system of tie-sets as it can be created a spanning tree expressed as thick links. Then, in Figure 2, L-transformation is conducted as follows:

$$L_3^{'} \leftarrow L_2 \oplus L_3, \quad L_6^{'} \leftarrow L_5 \oplus L_6.$$

As $L_3^{'}$ and $L_6^{'}$ are created by L-transformation, they are also independent tie-sets. However, we cannot find any spanning tree that forms the system of independent tie-sets $\left\{L_1, L_2, L_3^{'}, L_4, L_5, L_6^{'}\right\}$ after the L-transformation in Figure 2.

[§] $\oplus$ for a set A and a set B is defined as follows: $A \oplus B = (A - B) \cup (B - A) = (A \cup B) - (A \cap B)$.

DOI: 10.1002/cta

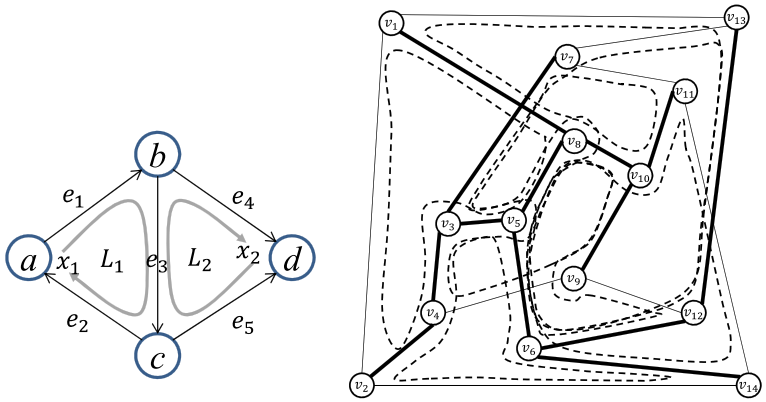

(a) In a planar graph (b) In a non-planar graph

Figure 1. Examples of a fundamental system of tie-sets. Thick and thin lines are links of a tree T and a co-tree $\overline{T}$, respectively.

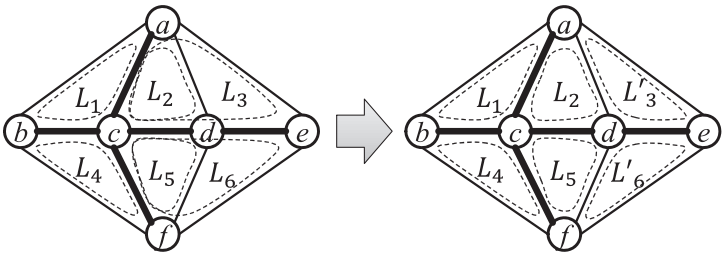

Figure 2. An example of a system of independent tie-sets that does not correspond to any fundamental system of tie-sets. Thick and thin lines are links of a tree T and a co-tree $\overline{T}$, respectively.

Let $\mathbb{L}'$ be the transformed system of tie-sets from $\mathbb{L}_B$ by replacing L_i by the L-transformation $L_i' \leftarrow L_i \oplus L_j$. Then, the following holds true between fundamental systems of tie-sets $\{\mathbb{L}_B\}$ and systems of independent tie-sets $\mathbb{L}'$.

$$\{\mathbb{L}_B\} \subseteq \{\mathbb{L}'\} \tag{7}$$

Therefore, by repeatedly conducting L-transformations, a system of independent tie-sets suitable for a target network management is obtained.

3.3. Problem formulation with tie-set currents

Let $x = (x_1, x_2, \ldots, x_\mu) \in \mathbb{R}^\mu$ denote the vector of tie-set currents that circulate along the tie-sets $\mathbb{L}_B = \{L_1, \ldots, , L_\mu\}$. Note that the tie-set currents have arbitrarily defined directions where $x_\lambda \geq 0$ if it is flowing in the same direction as the direction defined for L_λ, and $x_\lambda < 0$ otherwise. Let $B = [b_{k\lambda}] \in \mathbb{R}^{m \times \mu}$ be the *tie-set matrix* of the graph (V, E) with respect to $\mathbb{L}_B$, where

$$b_{k\lambda} = \begin{cases} 0 & e_k \notin L_\lambda \\ 1 & e_k \in L_\lambda \text{ and in the same direction with } x_\lambda \\ -1 & e_k \in L_\lambda \text{ and in the opposite direction with } x_\lambda. \end{cases}$$

DOI: 10.1002/cta

For example, $B=[b_{k\lambda}]$ in Figure 1(a) is

$$B=\begin{bmatrix}1 & 0\\ 1 & 0\\ 1 & -1\\ 0 & 1\\ 0 & -1\end{bmatrix}.$$

As stated earlier, in a mesh network, there are a subspace of solutions to (3) for a given J. Select an arbitrary solution of them, denoted by ξ, which is also called an *initial current vector*. Then, the current vector I can be expressed in terms of the tie-set currents x and the initial currents ξ as

$$I=Bx+\xi,$$

because one can easily show that $AB=0$. Then, P_G in (2) can be transformed into a function of tie-set currents:

$$\begin{aligned}P_G(x)&=(Bx+\xi)^TR^d(Bx+\xi)\\&=x^TB^TR^dBx^T+2\xi^TR^dBx+\xi^TR^d\xi\\&=x^TMx+2Nx+e,\end{aligned}$$

where $M:=B^TR^dB$, $N:=\xi^TR^dB$, and $e:=\xi^TR^d\xi$.

Given B, C, R, and ξ, the PLM problem, with respect to tie-set currents, is

$$\min_x P_G(x)=xMx^T+2xN+e \tag{8}$$

$$\text{s. t.}\quad -C\le Bx+\xi\le C. \tag{9}$$

As $P_G(x)$ is differentiable on $\mathbb{R}^\mu$, the necessary and sufficient condition for $x^*\in\mathbb{R}^\mu$ to be the optimal point of the PLM problem in (8) and (9) is that

$$\nabla P_G(x^*)=\left(\frac{\partial P_G(x^*)}{\partial x_1},\ldots,\frac{\partial P_G(x^*)}{\partial x_\mu}\right)=0. \tag{10}$$

Now, we define a power loss function $P_\lambda(x)$ with respect to a tie-set L_λ as

$$P_\lambda(x)=\sum_{e_k\in L_\lambda}p(i_k). \tag{11}$$

For each element of the vector, the following equation holds:

$$\frac{\partial P_G(x^*)}{\partial x_\lambda}=\sum_{e_k\in E}\frac{\partial p\left(i_k^*\right)}{\partial x_\lambda}=\sum_{e_k\in L_\lambda}\frac{\partial p\left(i_k^*\right)}{\partial x_\lambda}=\frac{\partial P_\lambda(x^*)}{\partial x_\lambda}=0. \tag{12}$$

According to (10), each power loss function $P_\lambda(x)$ with respect to a tie-set L_λ is minimum at $x=x^*$, that is,

$$\left(\frac{\partial P_0(x^*)}{\partial x_0},\frac{\partial P_1(x^*)}{\partial x_1},\ldots,\frac{\partial P_\mu(x^*)}{\partial x_\mu}\right)=0. \tag{13}$$

Equation (13) represents that if each power loss function $P_\lambda(x)$ with respect to L_λ is minimized, the overall power loss P_G becomes minimum as well. Therefore, local optimization with respect to μ-independent tie-sets must lead to the globally optimal solution.

DOI: 10.1002/cta

4. DISTRIBUTED CONTROL FOR POWER LOSS MINIMIZATION PROBLEM

4.1. Tie-set-based communications

Each node v_i has information of fundamental tie-sets to which v_i belongs as state information, which we call *tie-set information*. For example, node c in Figure 6 has $\{L_1, L_2\}$ as tie-set information. There is a leader node v_l^λ in each tie-set $L_\lambda \in \mathbb{L}_B$, and a leader node has *adjacent tie-sets* $\mathbb{L}_\lambda^a = \left\{L_1^\lambda, L_2^\lambda, \ldots\right\}$ defined as follows: Let $V(L_\lambda)$ be a set of all the vertices included in a tie-set L_λ. If $V(L_\lambda) \cap V(L_j) \neq \emptyset$, L_j is an adjacent tie-set of L_λ. For example, adjacent tie-sets of L_1 in Figure 6 is $\mathbb{L}_1^a = \{L_2\}$ so that L_1 constantly communicates with L_2. The mechanism of tie-set-based communication is introduced in [31] together with distributed algorithms based on tie-sets.

4.2. Tie-set-based autonomous distributed control model

To describe the procedure of *tie-set based autonomous distributed control* (TADiC), we use the notations and definitions of Table I. TADiC is conducted in a leader node in each tie-set asynchronously. A *tie-set agent* (TA) constantly navigates a tie-set L_λ to bring state information of L_λ to its leader node. TA includes a *measurement vector* (MV) $y_\lambda(t)$ that has the value of initial flows on edges in L_λ at time t. We define *tie-set evaluation function* (TEF) denoted as $\Phi(L_\lambda)$ to decide the process priority for overlapping resources shared by adjacent tie-sets. Here, we consider

$$\Phi(L_\lambda) = \left| \frac{d}{dx_\lambda} p_\lambda(x_\lambda) \right| \tag{14}$$

as TEF where $p_\lambda(x_\lambda)$ is defined in (21) in Section 4.3. Only when the process priority cannot be determined by the TEF in (14), we use $\Phi(L_\lambda) = \text{Random}$. TEF $\Phi(L_\lambda)$ is calculated on the basis of $y_\lambda(t)$ obtained by TA. *Tie-set flags* (TFs) denoted as $\zeta(L_\lambda)$ is used to distinguish tie-sets that are in process from tie-sets that are standby. >When $\zeta(L_\lambda) = 1$, L_λ is in process; otherwise, if $\zeta(L_\lambda) = 0$, L_λ is standby. The process priority is decided using *tie-set evaluation function message* (TEFM) that is sent to adjacent tie-sets $\mathbb{L}_\lambda^a = \left\{L_1^\lambda, L_2^\lambda, \ldots\right\}$ where the value of TEF $\Phi(L_\lambda)$ is written.

The procedure of TADiC is described as follows:

1. **Initialize**: In **Initialize**, TEF of a tie-set L_λ is set as $\Phi(L_\lambda) = 0$. TF of L_λ is also set as $\zeta(L_\lambda) = 0$. Then, L_λ calls **Send**.
2. **Send**: In **Send**, the value of TEF $\Phi(L_\lambda)$ is calculated on the basis of the current MV $y_\lambda(t)$ provided by TA with the value of L_λ's current flows ξ^λ defined in (18). After calculating $\Phi(L_\lambda)$, L_λ writes its TEF value into TEFM. Then, L_λ sends the TEFM to all the adjacent tie-sets $\mathbb{L}_\lambda^a$.
3. **Receive1**: **Receive1** is called when L_λ receives a TEFM after **Send**. In case that **Send** is not completed, TEFM is temporarily stored in the leader of L_λ. Until L_λ receives TEFMs from all the adjacent tie-sets $\mathbb{L}_\lambda^a$, L_λ waits for another TEFM. Then, L_λ calls **Compare**.
4. **Compare**: After receiving all the TEFMs form $\mathbb{L}_\lambda^a$, L_λ compares its value of $\Phi(L_\lambda)$ with the value of TEFs from adjacent tie-sets. If the value of $\Phi(L_\lambda)$ is the largest among those of all the adjacent

Table I. Notations and definitions for TADiC.

$\mathbb{L}_\lambda^a$	Adjacent tie-sets $\mathbb{L}_\lambda^a = \left\{L_j\right\}$. If $V(L_\lambda) \cap V(L_j) \neq \emptyset$, L_j is an adjacent tie-set of L_λ.
MV $y_\lambda(t)$	Measurement vector. MV $y_\lambda(t)$ contains various information of a node $v_i \in V(L_\lambda)$ at time t such as loads and renewables.
TA	Tie-set agent. An autonomous agent that constantly navigates a tie-set to bring the current MV $y_\lambda(t)$ with state info of L_λ to its leader node.
TEF $\Phi(L_\lambda)$	Tie-set evaluation function. A function that evaluates a tie-set based upon the current MV $y_\lambda(t)$ with certain predefined criteria.
TEFM	Tie-set evaluation function message. A message used to exchange the value of TEF $\Phi(L_\lambda)$ with adjacent tie-sets $\mathbb{L}_\lambda^a$.
TF $\zeta(L_\lambda)$	Tie-set flag. When $\zeta(L_\lambda) = 0$, a tie-set L_λ is standby; otherwise L_λ is in process ($\zeta(L_\lambda) = 1$).
TFS	Tie-set flag signal. A signal to notify the state of TF $\zeta(L_\lambda)$.

DOI: 10.1002/cta

tie-sets, L_λ sets its TF as $\zeta(L_\lambda)=1$; otherwise, $\zeta(L_\lambda)=0$. If the value of $\Phi(L_\lambda)$ is the same as $\Phi(L_j)$, L_λ uses another TEF $\Phi(L_\lambda)$ to decide the process priority such as $\Phi(L_\lambda)=$Random. Then, L_λ calls **Optimize**.

5. **Optimize**: If $\zeta(L_\lambda)=1$, L_λ conducts decentralized algorithm for power loss minimization (DAPLM) described in Algorithm 26. DAPLM is followed by setting its TF as $\zeta(L_\lambda)=0$. Then, L_λ calls **Notify**.
6. **Notify**: In **Notify**, L_λ sends a *tie-set flag signal* (TFS) to each adjacent tie-set $L_j \in \mathbb{L}_\lambda^a$ to notify that $\zeta(L_\lambda)=0$.
7. **Receive2**: **Receive2** is called when L_λ receives TFS after **Notify**. In case that **Notify** is not completed, TFS is temporarily stored in the leader of L_λ. Until L_λ receives TFS from all the adjacent tie-sets $\mathbb{L}_\lambda^a$, L_λ waits for another TFS. Then, L_λ calls **Confirm**.
8. **Confirm**: After receiving all the TFS form $\mathbb{L}_\lambda^a$, L_λ confirms that each TF of $L_j \in \mathbb{L}_\lambda^a$ is $\zeta(L_j)=0$. Then, L_λ calls **StandBy**.
9. **StandBy**: Let Δt be a communication interval among adjacent tie-sets. In **StandBy**, L_λ stands by for Δt to decide the speed of optimization. Then, L_λ calls **Send** again so that TADiC is iterated.

The flowchart of TADiC is described in Figure 3.

In **Send** and **Receive1** after **Initialize**, a leader node for a tie-set L_λ sends and receives TEFMs to decide whether it should be the one to recompute its current flows based on the magnitude of the TEF (the value of derivative of power loss in a tie-set) with respect to L_λ and the TEFs for all adjacent tie-sets $\mathbb{L}_\lambda^a$. To determine whether the magnitude of the TEF for L_λ is the maximum among all such tie-sets, the leader node for L_λ must receive the TEFM from the leader nodes of all adjacent tie-sets. According to the TADiC, failure to receive the TEFM from one or more leader nodes of adjacent tie-sets means that the leader node for L_λ simply stops, waits, and never again recomputes the current flows for L_λ. To make the TADiC sufficiently robust to recover from communications failures, we have a mechanism to cope with this type of failure. A leader node for L_λ polls a leader for an adjacent tie-set, if it has not received the TEFM from the adjacent leader node within a given amount of time and if no response is elicited from the poll, then it decides to proceed without the TEF information about that adjacent tie-set for this round.

In **Compare**, a leader node for tie-set L_λ determines that the magnitude of its TEF is the maximum among adjacent tie-sets to **Optimize** power flows. However, one or more adjacent tie-sets also might share the same the TEF values. According to the TADiC, the leader node for L_λ uses random choice to decide whether it should recompute the current flows for L_λ. The leader nodes for the adjacent tie-sets sharing the same TEF values for their tie-sets also need to determine whether they should recompute

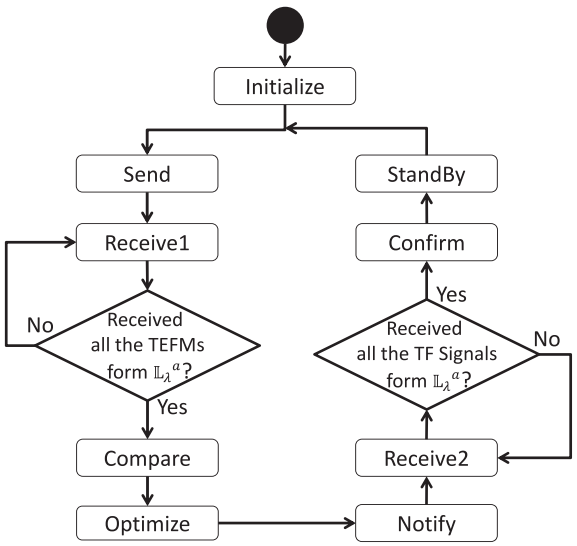

Figure 3. Tie-set based autonomous distributed control.

DOI: 10.1002/cta

the current flows for their tie-sets. If the leader nodes of the tie-sets with identical TEF values do not make a consistent decision on whether to recompute their respective currents, then it is possible that either leader nodes for some or all of these tie-sets recompute their currents at the same time or that none of the leader nodes for these tie-sets recomputes its currents. To specify a resolution technique that results in a consistent decision among tie-sets concerning computation of current flows in this case, we incorporate the algorithm to assign unique identifiers to leader nodes and to use them in resolving tie-sets in TEF values among adjacent tie-sets. This results in a consistent resolution of such tie-sets among leader nodes.

In **Notify** and **Receive2**, to proceed to the **StandBy** state via **Confirm**, the leader node for a tie-set L_λ must receive from the leader nodes of all adjacent tie-sets the TFS (flag value) indicating that they are ready to continue. If the leader node for L_λ fails to receive flags from the leader nodes of one or more adjacent tie-sets, it exploits the polling method that is the same mechanism used in **Send** and **Receive1**.

4.3. Decentralized algorithm for power loss minimization

Decentralized algorithm for PLM (*DAPLM*) is described in Algorithm 26 and called by TADiC in Figure 3.

Let γ be the number of edges in a tie-set $L_\lambda = \{e_1, e_2, \ldots, e_\gamma\}$ where $\gamma = |L_\lambda|$. Then, we define the following:

$$B_\lambda = \left(b_{\lambda 1}, b_{\lambda 2} \ldots, b_{\lambda\gamma}\right), \tag{15}$$

$$I_\lambda = \left(i_1, i_2 \ldots, i_\gamma\right), \tag{16}$$

$$R_\lambda = \left(r_1, r_2 \ldots, r_\gamma\right), \tag{17}$$

$$\xi^\lambda = \left(\xi_1, \xi_2 \ldots, \xi_\gamma\right). \tag{18}$$

With respect to a tie-set flow x_λ of L_λ, the electric current vector I_λ of L_λ is defined as follows:

$$I_\lambda = x_\lambda B_\lambda + \xi^\lambda \tag{19}$$

Let $p_\lambda(x_\lambda)$ be a *tie-set power loss* (TPL) function of a tie-set L_λ as

$$p_\lambda(x_\lambda) = I_\lambda^T R_\lambda^d I_\lambda \tag{20}$$

where $R_\lambda^d = \mathrm{diag}\left(r_1, , r_2, \ldots, , r_\gamma\right)$ is a diagonal matrix whose elements are $R_\lambda = (r_1, r_2, \ldots, r_\gamma)$. On the basis of definitions (15–20), the TPL function $p_\lambda(x_\lambda)$ is

$$p_\lambda(x_\lambda) = \sum_{e_k \in L_\lambda} r_k (b_{\lambda k} x_\lambda + \xi_k)^2. \tag{21}$$

In STEP 0, DAPLM initializes the value of a current tie-set flow x_λ of L_λ as 0. The information of current edge flows ξ^λ on L_λ is provided by MV $y_\lambda(t)$ on TA.

In STEP 1, DAPLM calculates the optimal tie-set flow x_λ to satisfy

$$\begin{aligned} \frac{d}{dx_\lambda} p_\lambda(x_\lambda) &= \frac{d}{dx_\lambda} \sum_{e_k \in L_\lambda} r_k (b_{\lambda k} x_\lambda + \xi_k)^2 \\ &= \sum_{e_k \in L_\lambda} \frac{d}{dx_\lambda} r_k (b_{\lambda k} x_\lambda + \xi_k)^2 \\ &= 0 \end{aligned} \tag{22}$$

that is,

$$x_\lambda = -\frac{\sum_{e_k \in L_\lambda} r_k b_{\lambda k} \xi_k}{\sum_{e_k \in L_\lambda} r_k} \tag{23}$$

because $b_{\lambda k}^2 = 1$.

DOI: 10.1002/cta

In STEP 2, each edge flow $i_k \in I_\lambda$ is updated to $b_{\lambda k}x_\lambda + \xi_k$ where edge flows on L_λ are optimized to minimize the power loss in L_λ.

An example of DAPLM is shown in Figure 4. In the tie-set $L_\lambda = \{e_1(b,a), e_2(a,c), e_3(c,b)\}$ in Figure 4,

$$\begin{aligned} B_\lambda &= (b_{\lambda 1}, b_{\lambda 2}, b_{\lambda 3}) = (1,1,1), \\ \xi^\lambda &= (\xi_1, \xi_2, \xi_3) = (9.0, 9.0, 2.0), \\ R_\lambda &= (r_1, r_2, r_3) = (0.2, 0.1, 0.05). \end{aligned}$$

Algorithm 1 Decentralized Algorithm for Power Loss Minimization (DAPLM)

STEP 0:
Initialize a current tie-set flow x_λ of L_λ as 0.
Obtain ξ^λ provided by MV $y_\lambda(t)$ on TA.
STEP 1:
Calculate x_λ according to (23).
STEP 2:
for each i_k on $e_k \in L_\lambda$ **do**
Update an electric current i_k to $b_{\lambda k}x_\lambda + \xi_k$.
Inject the minimized lost power $r_k {i_k}^2$ at the destination node of the current i_k.
end for

According to (21), the TPF function in L_λ is

$$\begin{aligned} p_\lambda(x_\lambda) &= r_1(b_{\lambda 1}x_\lambda + \xi_1)^2 + r_2(b_{\lambda 2}x_\lambda + \xi_2)^2 + r_3(b_{\lambda 3}x_\lambda + \xi_3)^2 \\ &= 0.2 \times (1 \cdot x_\lambda + 9.0)^2 + 0.1 \times (1 \cdot x_\lambda + 9.0)^2 + 0.05 \times (1 \cdot x_\lambda + 2.0)^2 \\ &= 0.35x_\lambda^2 + 5.6x_\lambda + 24.5. \end{aligned}$$

In STEP 0, tie-set flow x_λ is initialized to 0; the value of TPL function is $p_\lambda(0) = 24.5$. In STEP 1, the optimal x_λ is calculated according to (23) as follows:

$$\begin{aligned} x_\lambda &= -\frac{r_1 b_{\lambda 1}\xi_1 + r_2 b_{\lambda 2}\xi_2 + r_3 b_{\lambda 3}\xi_3}{r_1 + r_2 + r_3} \\ &= -\frac{(0.2 \cdot 1 \cdot 9.0) + (0.1 \cdot 1 \cdot 9.0) + (0.05 \cdot 1 \cdot 2.0)}{0.2 + 0.1 + 0.05} \\ &= -8.0. \end{aligned}$$

Then, the currents are updated in STEP 2 as

$$\begin{aligned} i_1 &= b_{\lambda 1}x_\lambda + \xi_1 = 1 \cdot (-8.0) + 9.0 = 1.0 \\ i_2 &= b_{\lambda 2}x_\lambda + \xi_2 = 1 \cdot (-8.0) + 9.0 = 1.0 \\ i_3 &= b_{\lambda 3}x_\lambda + \xi_3 = 1 \cdot (-8.0) + 2.0 = -6.0 \end{aligned}$$

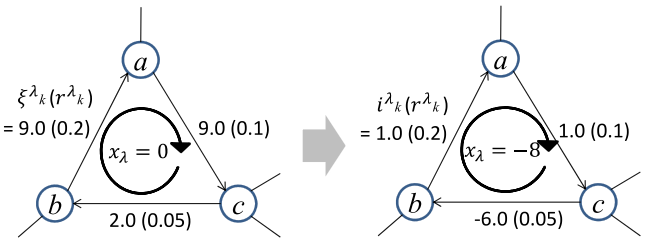

Figure 4. Example for DAPLM.

DOI: 10.1002/cta

so that the current vector in L_λ is

$$I_\lambda = (i_1, i_2, i_3) = (1.0, 1.0, -6.0).$$

In summary, the power flow loss in L_λ of Figure 4 before conducting DAPLM is $p_\lambda(0) = 24.5$, and the loss after DAPLM is $p_\lambda(-8.0) = 2.1$ where the lost power $0.2 \times 1.0^2 = 0.2$ (W) on the link $e(b, a)$ is injected at node a, and the lost power $0.1 \times 1.0^2 + 0.05 \times (-6.0)^2 = 1.9$ (W) on the links $e(a, c)$ and $e(c, b)$ is injected at node c.

5. SIMULATION AND EXPERIMENTS

The PLM problem can be solved through local optimizations in a system of μ-independent tie-sets that are equivalent to μ-dimensional linear vector space as discussed in Section 3.1. By conducting the decentralized algorithms described in Section 4, optimal flows that minimize the power line loss of a graph can be obtained. To verify this property and conduct experiments as well as compare it with a centralized approach, we made a simulator in Java where all the distributed algorithms to solve the PLM problem are implemented. We exploited Java Universal Network/Graph Framework [32], which is a software library that provides a common and extensible language for the modeling, analysis, and visualization of data that can be represented as a graph or network. Common buffering method and polling method are employed in a simulation node. Then, we run the simulator using OS Windows 7 as a simulation environment.

In this experiment, each link capacity is $c_k = 100$ (A) ($k = 1, 2, \ldots, m$). Tie-sets exchange $\Phi(L_\lambda) = \left|\frac{d}{dx_\lambda} p_\lambda(x_\lambda)\right|$ as TEF, and every MV $y_\lambda(t)$ is constantly sent to a leader node of each tie-set. Communication Interval in StandBy in Figure 3 is $\Delta t = 1$ ms in this simulation. When all the tie-sets satisfy the following termination condition, simulation procedure stops.

$$-0.1 < \frac{d}{dx_\lambda} p_\lambda(x_\lambda) < 0.1. \tag{24}$$

5.1. Experiments using IEEE bus test systems

In this experiment, the simulation network $G = (V, E)$ and its properties are given on the basis of IEEE bus test systems with 14, 30, 57, and 118 buses, and 20, 41, 78, and 179 lines, respectively. The number of tie-sets in 14-bus, 30-bus, 57-bus, and 118-bus systems is 7, 12, 22, and 62, respectively. The sets of link resistances, generators, and loads are provided by the IEEE bus systems. We create fundamental systems of tie-sets on the bus systems in a distributed manner. The initial flow ξ_k of each edge is randomly assigned with $-50 \le \xi_k \le 50$ (A). Experimental data are taken when every tie-set satisfies (24) and conducted 10 times from the section below so that the average value is calculated.

5.1.1. Optimized edge flows. Figure 5 shows the values of edge flows (electric currents (A)) on $e_k \in E$ before and after optimization in the 14-bus, 30-bus, 57-bus, and 118-bus grids. In Figure 5, edge flows are sorted in ascending order. All the edge flows are balanced to minimize the power loss of G by iteratively updating the tie-set flow x_λ in each tie-set L_λ. From Figure 5, edge flows in the 118-bus system are more balanced as the grid has the larger number of links compared with other bus systems.

5.1.2. Current distribution based on resistance. Figure 6 is another way of showing edge flows on resistances $r_k \in R$ sorted in ascending order. As indicated in Figure 6, the variance of optimized edge flows is larger on smaller resistances and smaller on lager resistances, which means the large amount of edge flows pass through links whose resistances are small.

5.1.3. Optimized power flow losses. Figure 7 shows the power loss (W) on each edge sorted in ascending order as well. With the optimized edge flows, the power loss of every link is minimized. This result demonstrates that individual power losses on edges by optimized flows are almost half of the losses by initial flows.

DOI: 10.1002/cta

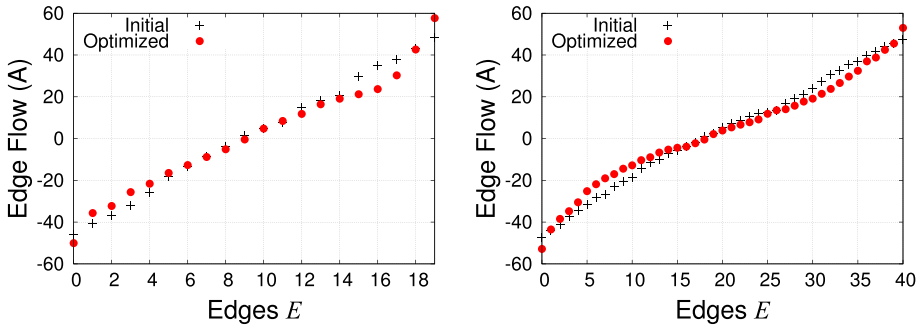

(a) 14-bus system. (b) 30-bus system.

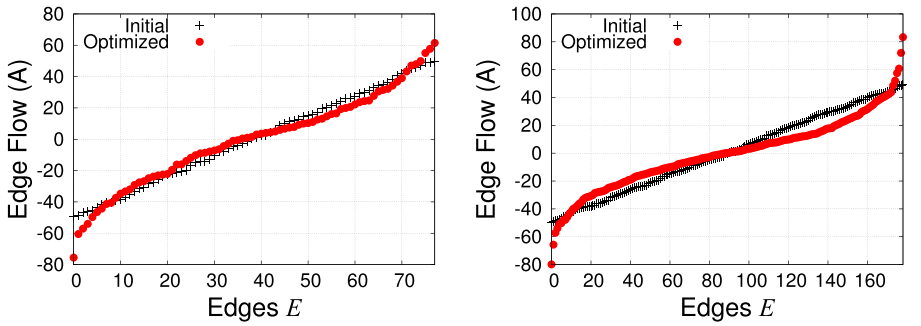

(c) 57-bus system. (d) 118-bus system.

Figure 5. Edge flows i_k on edges $e_k \in E$ before and after optimization in the IEEE bus test systems.

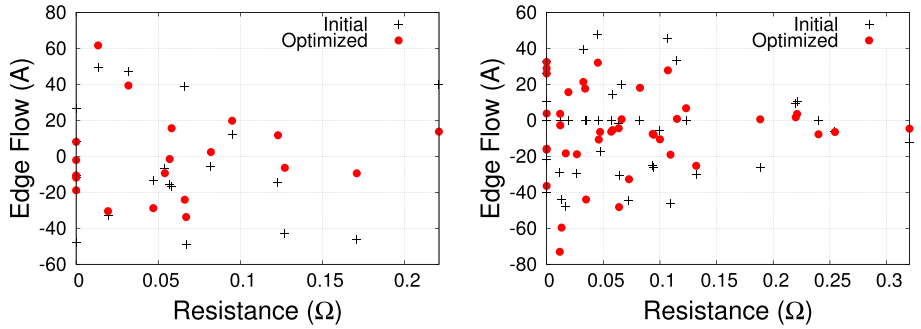

(a) 14-bus system. (b) 30-bus system.

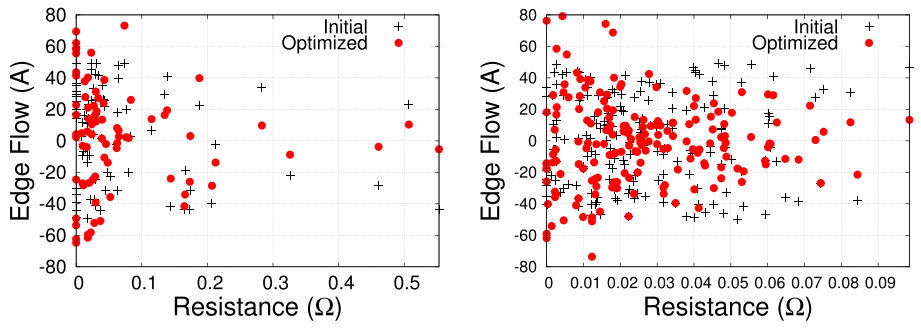

(c) 57-bus system. (d) 118-bus system.

Figure 6. Edge flows i_k sorted by resistances r_k on edges $e_k \in E$ before and after optimization in the IEEE bus test systems.

DOI: 10.1002/cta

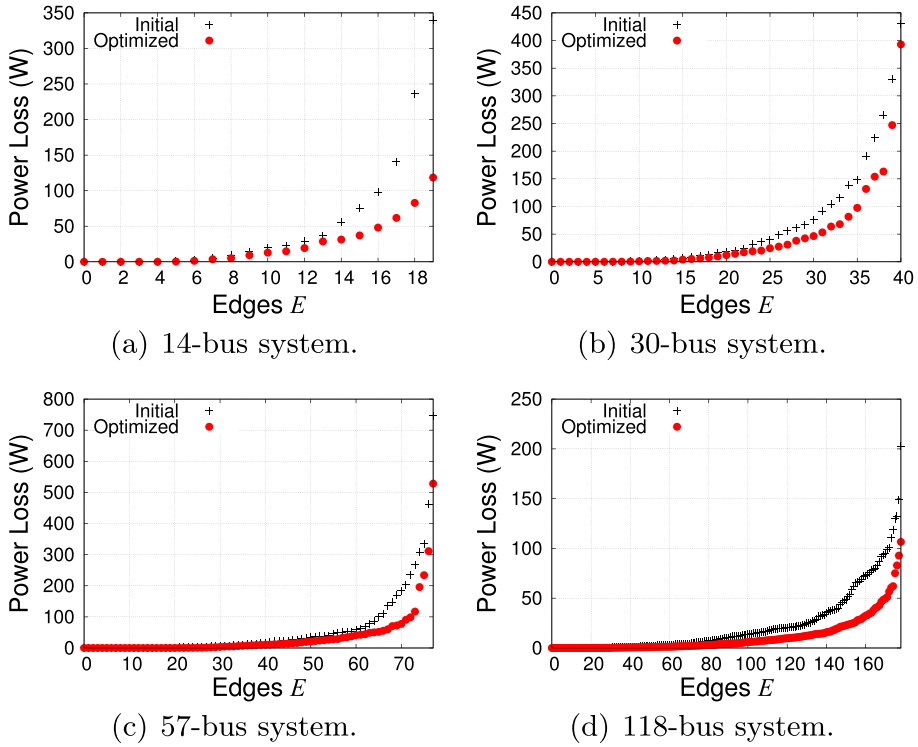

Figure 7. Power losses p_k on edges $e_k \in E$ before and after optimization in the IEEE bus test systems.

5.1.4. Total power loss by initial and optimized flows. Table II shows the results of the total power loss by initial and OPFs with IEEE 14-bus, 30-bus, 57-bus, and 118-bus systems. Those data are taken 10 times, and the averaged value has been calculated. In Table II, 'Initial P_G' represents the total power loss by not-optimized power flows on all the edges of a graph, and 'Optimal P_G' represents the total power loss by optimized power flows.

As suggested in Table II, the optimal flows in 14-bus and 118-bus systems achieve about a 50% reduction of power loss. As to 30-bus and 57-bus systems, more than a 30% reduction of power loss has been realized.

5.1.5. Analysis on property performance. Now, we analyze the property performance of the proposed decentralized algorithm. In Figure 8, the number of computations for TADiC and DAPLM at each time step is provided in the IEEE bus systems. As indicated in Figure 8, all the tie-sets of 17-bus, 30-bus, 57-bus, and 118-bus system stop their procedures (TADiC and DAPLM) when $t = 130$, 175, 156, and 323 ms, respectively, as they satisfy (24). The behaviors of those results show that the proposed method conducts many times of both TADiC and DAPLM until about 100 ms and then reduces the computations after 100 ms. This result shows that distributed optimization technique based on tie-sets tries to realize overall optimization quickly and then continues its procedures until it converges to satisfy (24).

As to communications complexity $\Gamma(t)$ at time t, which is the number of messages used in conducting TADiC, we can calculate it with $\Gamma(t) = 2 \times \alpha(t) \times \sum_{L_\lambda \in \mathbb{L}_B} \left|\mathbb{L}_\lambda^a\right|$ where $\alpha(t)$ is the total number of

Table II. The total power loss by initial and optimized flows with IEEE bus test systems.

	14 buses	30 buses	57 buses	118 buses
Initial P_G (W)	888.055	2586.321	4708.256	3980.594
Optimal P_G (W)	413.982	1786.854	2938.289	2023.729

DOI: 10.1002/cta

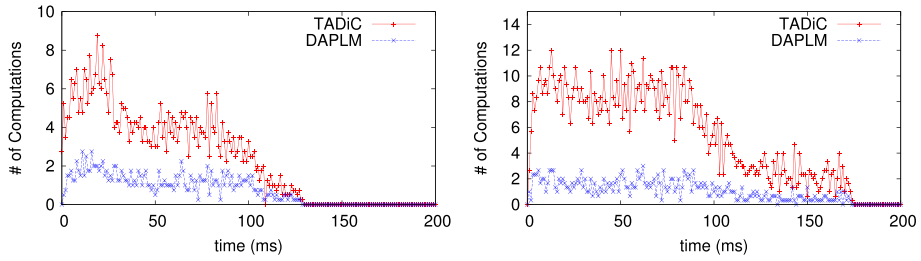

(a) 14-bus system. (b) 30-bus system.

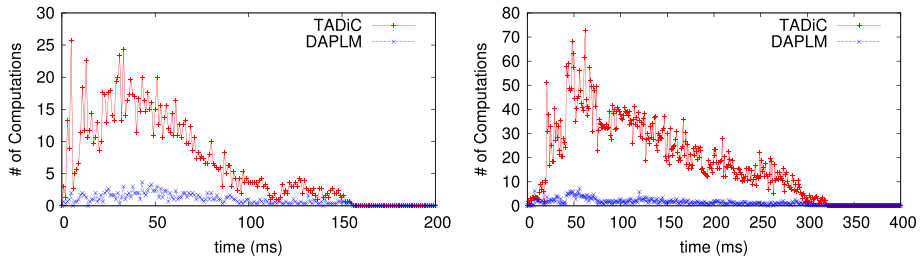

(c) 57-bus system. (d) 118-bus system.

Figure 8. The number of computations of TADiC and DAPLM at every time step in the IEEE bus systems.

computations by TADiC at time t. For example, in the IEEE 30-bus system used in this simulations, the communications complexity is $\Gamma(10) = 2 \times 8 \times 84 = 1344$ where $\alpha(10) = 8$ and $\sum_{L_i \in \mathbb{L}_B} \left| \mathbb{L}_d^a \alpha(10) \right| = 84$.

5.2. *Comparison with centralized optimization*

In this experiment, we show the effectiveness of the decentralized algorithm based on tie-sets by comparing convergence speed with the centralized optimization approach. The centralized approach sequentially optimizes flows by picking a tie-set whose TEF is the largest among all the tie-sets. Initial flows are randomly given to all the edges E of G with $-50 \leq \xi_k \leq 50$ $(k = 1, 2, \ldots, m)$.

Figure 9 shows the result of the comparison experiment about the convergence speed in the IEEE 118-bus grid and a 100-bus grid with random link connections. In the 100-bus grid, each link resistance r_k is randomly given between 0 to 0.5 (Ω). As clearly shown in Figure 9, the decentralized algorithm based on tie-sets demonstrated fast convergence than the centralized scheme. This is because the decentralized method realizes parallel optimizations by communicating with adjacent tie-sets, whereas the centralized method collects all the data of current flows from each node to conduct optimization. Because the distributed algorithm shows its fast convergence nature, the result also

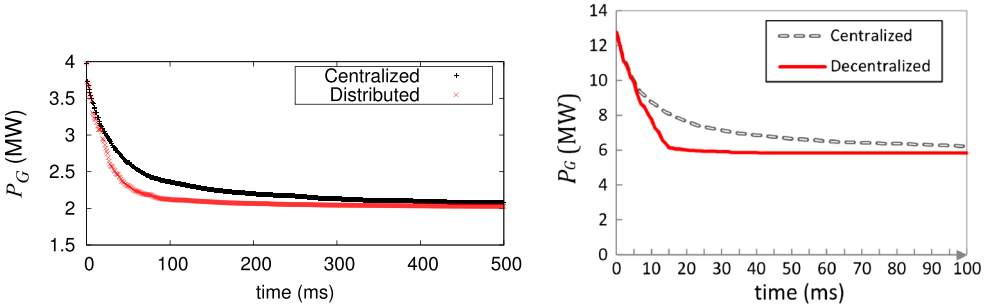

(a) IEEE 118-bus system. (b) 100-bus grid with random link connections.

Figure 9. Comparison of convergence of power loss P_G with centralized optimization in IEEE 118-bus and 100-bus grids.

DOI: 10.1002/cta

suggests that centralized systems should be replaced by autonomous distributed systems to realize efficient parallel computation in a future power network where power flows are constantly updated with stochastic process of loads and renewables.

5.3. *Performance in different topologies*

We have analyzed the specific grids using IEEE bus test systems. Therefore, we analyze the nature of the proposed optimization method using random mesh topologies with different size of nodes and edges. Initial flows are given to all the edges E of G with $-50 \leq \xi_k \leq 50$ $(k = 1, 2, \ldots \ldots, m)$ (A). Experiment data are taken when all the tie-sets satisfy (24). We conducted 20 experiments for each simulation network to calculate the average value.

5.3.1. Power loss with different number of links. In this experiment, we conducted a simulation to examine the power loss P_G of an entire graph with the different number of edges with a 100-bus grid where $|E| = 100, 200, 300, 400,$ and 500. Each link resistance r_k is randomly given between 0 to 0.1 (Ω).

As seen in Figure 10, the total power loss P_G by initial (not-optimized) flows shows large increase at a rate proportional to the number of edges, whereas the loss by optimized flows shows a subtle decrease as the number of edges increases. The delta between the loss by initial flows and optimized flows significantly increases as the number of power lines becomes larger. This result indicates that the larger the number of lines becomes, the more amount of the power loss we can reduce. However, we need to consider the cost of installing power lines when we configure a power network.

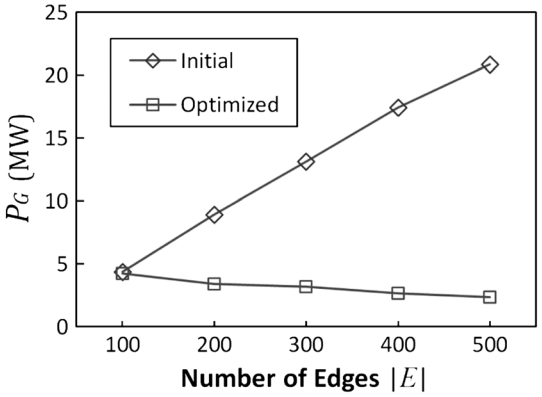

Figure 10. Power loss P_G with the different number of edges (100 to 500) with a 100-bus grid.

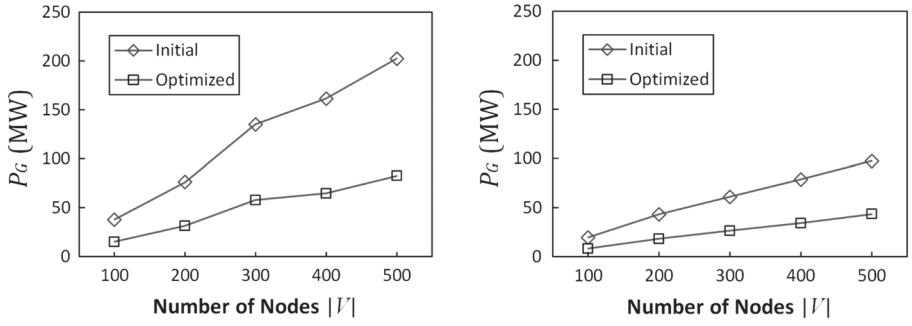

(a) Initial flows are given to all the edges E of G.

(b) Initial flows are only given to the edges of tree T of G.

Figure 11. The total power loss P_G with the different number of nodes (100 to 500).

DOI: 10.1002/cta

5.3.2. Power loss with different network sizes. Next, we conducted a simulation to look at the power loss P_G of an entire graph with the different number of nodes where $|V| = 100, 200, 300, 400$, and 500 with the number of links $|E| \approx 200, 400, 600, 800$, and 1000. Each link resistance r_k is randomly given between 0 to 0.5 (Ω).

In the experiment shown in Figure 11(a), initial edge flows are given to all the edges E of G, whereas initial flows in Figure 11(b) are only given to the edges of tree T of G. Figure 11(a) indicates that the power loss P_G is proportionate to the number of nodes and the total loss by optimized flows is less than the half of the total loss by initial (not-optimized) flows. Figure 11(b) shows similar tendency to the result of Figure 11(a). From the result shown in Figure 11(b), the traditional tree or bus topology is quite inefficient for future grids with bi-directional flows. This result gives rise to use of mesh topologies to future power networks.

6. CONCLUSION AND FUTURE WORK

In this paper, a PLM problem is first formulated on the basis of tie-set graph theory to distribute electricity with optimized link flows targeting prospective future grids. Then, we proposed the decentralized algorithms based on tie-sets that represent loops in a power network to solve the PLM problem and described how to realize autonomous distributed control with autonomous agents navigating the tie-sets. The simulation results show that local optimizations constantly iterated within a fundamental system of tie-sets calculate optimal edge flows of entire grids based on the IEEE bus test systems. The results also show that the proposed method realizes more than a 50% reduction of power loss for a grid with 100 to 500 nodes.

Here, we list up the future work to be studied as follows:

- Integration of the proposed model with optimal real-time power flow models that are also being developed to compensate the renewable intermittency by using battery systems.
- Study on whether the uniqueness of tie-sets can be used to study the uniqueness of optimal solution and whether there is any connection between the method based on tie-sets and the previous methods as in [25, 26].
- Comprehensive analyses of all the proposed decentralized algorithms and comparison of time complexity, communication complexity, and space complexity of the proposed method with those of other existing known techniques.
- Finding what factor(s) of the proposed model affect the speed of convergence and preciseness of the optimized outcome of the total power loss compared with theoretical limitation.
- Proof that the optimized power loss converges on the solution with certain error range by iterative power-loss minimization based on tie-sets.

ACKNOWLEDGEMENT

The authors would like to thank Prof. Steven Low in EE and CMS at Caltech for his invaluable comments and suggestions.

REFERENCES

1. Locke G, Gallagher PD. NIST framework and roadmap for smart grid interoperability standards. Tech. rep., National Institute of Standards and Technology, Jan. 2010.
2. Hui S, Chung H-H, Yip S-C. A bidirectional AC–DC power converter with power factor correction. *IEEE Transactions on Power Electronics* 2000; **15**(5):942–948.
3. Galli S, Scaglione A, Wang Z. For the grid and through the grid: the role of power line communications in the smart grid. *Proceedings of the IEEE* 2011; **99**(6):998–1027.
4. Wang Z, Scaglione A, Thomas R. Generating statistically correct random topologies for testing smart grid communication and control networks. *IEEE Transactions on Smart Grid* 2010; **1**(1):28–39.
5. Mosaic PC. Mesh networks is communications winner in utility survey. 2009.
6. Lavaei J, Low S. Relationship between power loss and network topology in power systems. In *49th IEEE Conference on Decision and Control* (*CDC*), 2010; 4004–4011.
7. Fujisawa T. Maximal flow in a lossy network. In *Proc. of First Annual Allerton Conference on Circuit and System Theory*, 1963; 385–393.

DOI: 10.1002/cta

8. Iri M, Shirakawa I, Kajitani Y, Shinoda S. Graph Theory with Exercises. Japan: CORONA Pub, 1983.
9. Lukman D, Blackburn TR. Loss minimization in load flow simulation in power system. In *Proc. of 2001 4th IEEE International Conference on Power Electronics and Drive Systems*, vol. **1**, 2001; 84–88.
10. Saino R, Takeshita T, Izuhara N, Ueda F. Power flow estimation and line-loss-minimization control using UPFC in loop distribution system. In *IEEE 6th International on Power Electronics and Motion Control Conference* (*IPEMC*), 2009; 2426–2431.
11. Stevenson WD. Elements of Power System Analysis-4/E. McGraw-Hill Book Company Inc.: New York, 1982.
12. Koide T, Kubo H, Watanabe H. A study on the tie-set graph theory and network flow optimization problems. *International Journal of Circuit Theory and Applications* 2004; **32**(6):447–470.
13. Huneault M, Galiana F. A survey of the optimal power flow literature. *IEEE Transactions on Power Systems* 1991; **6**(2):762–770.
14. Carpentier J. Contribution to the economic dispatch problem. *Bulletin de la Societe Francoise des Electriciens* 1962; **3**(8):431–447.
15. Bergen AR. Power Systems Analysis, 2/E. Pearson Education: India, 2009.
16. Lin W-M, Huang C-H, Zhan T-S. A hybrid current–power optimal power flow technique. *IEEE Transactions on Power Systems* 2008; **23**(1):177–185.
17. Jiang Q, Chiang N, Guo C, Cao Y. Power-current hybrid rectangular formulation for interior-point optimal power flow. *Generation, Transmission Distribution, IET* 2009; **3**(8):748–756.
18. Jiang Q, Geng G, Guo C, Cao Y. An efficient implementation of automatic differentiation in interior point optimal power flow. *IEEE Transactions on Power Systems* 2010; **25**(1):147–155.
19. Jabr R. Radial distribution load flow using conic programming. *IEEE Transactions on Power Systems* 2006; **21**(3): 1458–1459.
20. Christie R, Wollenberg B, Wangensteen I. Transmission management in the deregulated environment. *Proceedings of the IEEE* 2000; **88**(2):170–195.
21. Aguado J, Quintana V. Inter-utilities power-exchange coordination: a market-oriented approach. *IEEE Transactions on Power Systems* 2001; **16**(3):513–519.
22. Conejo A, Aguado J. Multi-area coordinated decentralized DC optimal power flow. *IEEE Transactions on Power Systems* 1998; **13**(4):1272–1278.
23. Jabr R. Optimal power flow using an extended conic quadratic formulation. *IEEE Transactions on Power Systems* 2008; **23**(3):1000–1008.
24. Lavaei J, Babakhani A, Hajimiri A, Doyle J. Solving large-scale linear circuit problems via convex optimization. In *Proceedings of IEEE Conference on Decision and Control*, 2009; 4977–4984.
25. Tan CW, Cai D, Lou X. DC optimal power flow: uniqueness and algorithms. In *IEEE Third International Conference on Smart Grid Communications* (*SmartGridComm*), 2012; 641–646.
26. Lavaei J, Low S. Zero duality gap in optimal power flow problem. *IEEE Transactions on Power Systems* 2012; **27**(1):92–107.
27. Mieghem V. Graph Spectra for Complex Networks. Cambridge University Press: New York, 2011.
28. Shinomiya N, Koide T, Watanabe H. A theory of tie-set graph and its application to information network management. *International Journal of Circuit Theory and Applications* 2001; **29**(4):367–379.
29. Nakayama K, Benson K, Bic L, Dillencourt M. Complete automation of future grid for optimal real-time distribution of renewables. In *IEEE Third International Conference on Smart Grid Communications* (*SmartGridComm*), 2012; 418–423.
30. Nakayama K, Shinomiya N, Watanabe H. An autonomous distributed control method for link failure based on tie-set graph theory. *IEEE Transactions on Circuits and Systems I: Regular Papers* 2012; **59**(11):2727–2737.
31. Nakayama K, Shinomiya N, Watanabe H. An autonomous distributed control method based on tie-set graph theory in future grid. *International Journal of Circuit Theory and Applications* 2013; **41**(11):1154–1174.
32. O'Madadhain J, Fisher D, Nelson T. JUNG: Java universal network/graph framework. Website. (Available from: http://jung.sourceforge.net/) [accessed on 24 January 2010].

DOI: 10.1002/cta